Available online at www.sciencedirect.com
SCIENCE DIRECT®

Journal of the European Ceramic Society 24 (2004) 627–634

www.elsevier.com/locate/jeurceramsoc

Characterization of alumina–3 wt.% titania coating prepared by plasma spraying of nanostructured powders

Xinhua Lin[a,*], Yi Zeng[a], Soo Who Lee[b], Chuanxian Ding[a]

[a]*Shanghai Institute of Ceramics, Chinese Academy of Sciences, 1295 Dingxi Road, Shanghai 200050, PR China*
[b]*Sun Moon University, Department of Material Engineering, Asan, South Korea*

Received 11 November 2002; received in revised form 4 March 2003; accepted 15 March 2003

Abstract

Nanostructured and conventional alumina–3 wt.% titania coatings were deposited by air plasma spraying (APS). The microstructure and phase composition of the coatings were characterized by X-ray diffraction (XRD), scanning electron microscopy (SEM) and transmission electron microscopy (TEM). Mechanical properties including hardness, adhesion strength, crack extension force (G_C) and sliding wear rate were measured. Equiaxed α-Al_2O_3 grains were observed in the nanostructured Al_2O_3–3 wt.% TiO_2 coating and the diameter of α-Al_2O_3 grains were about 150 to 700 nm in size. The microhardness of both kinds of coating was similar and about 820 $HV_{0.2}$. However, the adhesion strength and crack extension force of the nanostructured coating increased by 33 and 80%, respectively, as compared with those of the conventional coating. The wear rate of the nanostructured coating was lower than that of the conventional coating. The results were explained in terms of characteristics of the powders and microstructure of the coatings.

Keywords: Plasma spraying; Coatings; $A1_2O_3$–TiO_2; Adhesion strength; Wear resistance

1. Introduction

Materials with fine-scale microstructures have long been recognized to exhibit remarkable and technologically attractive properties including mechanical, magnetic, electrical and optical properties.[1] The mechanical property plays an important role among them, especially for ceramic materials. Nanostructured materials possess higher hardness, toughness and wear resistance.[2–5] The wear of n-WC/Co bulk materials was about 60% of that of conventional counterparts.[3] The unindented strength of Al_2O_3–5 vol.% SiC nanocomposite increased by about fourfold compared to pure Al_2O_3.[4]

Nanostructured coatings were also expected to have improved mechanical properties and may be the first nanostructured materials to find commercial application.[6] There is a growing interest in the preparation of nanostructured coatings. Many methods, such as CVD, PVD and sol-gel, have been developed to deposit nanostructured coatings. Recently, some studies[6–10] reported that nanostructured coatings were prepared by thermal spraying with micro-sized nanostructured powder, which was obtained by agglomerating individual nanoparticles using spray drying.

Plasma sprayed alumina-based ceramic coatings are used in a variety of applications to provide electrical insulation, increased wear resistance, and chemically unreactive surfaces.[11] In this paper, nanostructured alumina–3 wt.% titania coating was deposited by plasma spraying reconstituted nano-sized alumina and titania powder. For comparison, the corresponding conventional alumina–3 wt.% titania coating was also prepared with the conventional fused and crushed powder. The thickness of both coatings was about 300 μm. The microstructure and some mechanical properties of these coatings were examined.

2. Experimental

2.1. Preparation of coatings

Nano-sized Al_2O_3 and TiO_2 powders, with a mean diameter of 70 and 80 nm were selected as raw feedstock

* Corresponding author. Tel.: +86-21-52412990; fax: +86-21-52413903.
E-mail address: 1_xh201@sina.com (X. Lin).

0955-2219/03/$ - see front matter © 2003 Elsevier Ltd. All rights reserved.
doi:10.1016/S0955-2219(03)00254-1

for this study, and were supplied by Hunan Biasfree Corp. (China). The nano-sized alumina and titania powders were reconstituted into micrometer-sized granules with composition equivalent to the conventional Al_2O_3–3 wt.% TiO_2 powder by spray drying. The granules obtained in this way were subsequently sintered in a furnace in order to be densified. This reconstituted powder had good flowability for plasma spraying. The morphologies of both Al_2O_3–3 wt.% TiO_2 powders are shown in Fig. 1. The nanostructured granules were spherical and porous with size ranging from 11 to 45 μm. The conventional powder exhibited an angular and irregular morphology with size between 10 and 35 μm.

Coatings were deposited using a Sulzer-Metco F4 plasma torch under atmospheric conditions (APS-2000). Stainless steel coupons were used as substrates. Before spraying, the substrates were degreased and grit blasted with white corundum. A mixture of argon and hydrogen was used as the plasma gas. Powder stored in a powder feeder (Twin-system 10-C) was injected into the plasma jet by argon gas. Compressed air was used as the cooling gas during plasma spraying. The typical spraying parameters for both conventional and nanostructured Al_2O_3–3 wt.% TiO_2 coatings are summarized in Table 1.

Table 1
Summary of the plasma spraying parameters

Parameters	Nanostructured coating	Conventional coating
Arc current, A	650	530
Arc voltage, V	62	72
Primary plasma gas (Ar), slpm	41	41
Auxiliary plasma gas (H_2), slpm	14	14
Carrier gas (Ar), slpm	3.5	3.5
Feeding distance, mm	6	6
Powder injector diameter, mm	1.8	1.8
Nozzle diameter, mm	6	6
Spray distance, mm	100	120

2.2. Characterization of coatings

The phase composition of the as-sprayed samples was determined by X-ray diffraction (XRD) with nickel filtered CuKα ($\lambda = 1.54056$) radiation on a Rigaku D/Max2550 diffractometer and microstructure of the as-sprayed coatings was examined using field emission scanning electron microscope (JSM-6700F, JEOL, Japan) and transmission electron microscope (JEM-2000X, JEOL, Japan), respectively.

Porosity of the coatings was estimated by quantitative image analysis. Ten fields are selected for the measurement of porosity. The microhardness and crack extension force measurements were conducted on the cross section of the as-sprayed coatings using Vickers Indentor with the loads of 200 and 1000 g applied respectively for 15 s. The measurement of the crack extension force has been described elsewhere.[12] Adhesion strength of coatings was evaluated according to ASTM C 633-79. A sliding, reciprocating and vibrating test machine was used for friction and wear tests. The detailed wear experiment was described in a previous work.[9]

3. Results and discussions

3.1. Phase composition of coatings

The XRD patterns of Al_2O_3–3 wt.% TiO_2 powders and coatings are shown in Fig. 2. The trigonal α-Al_2O_3 appeared in the nanostructured and conventional

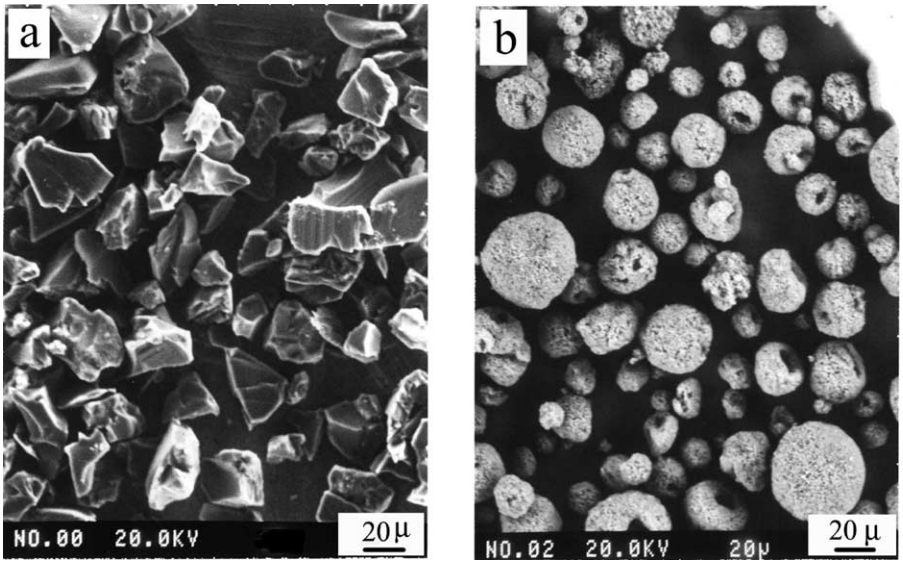

Fig. 1. Morphologies of the Al_2O_3–3 wt.% TiO_2 powders: (a) conventional; (b) nanostructured.

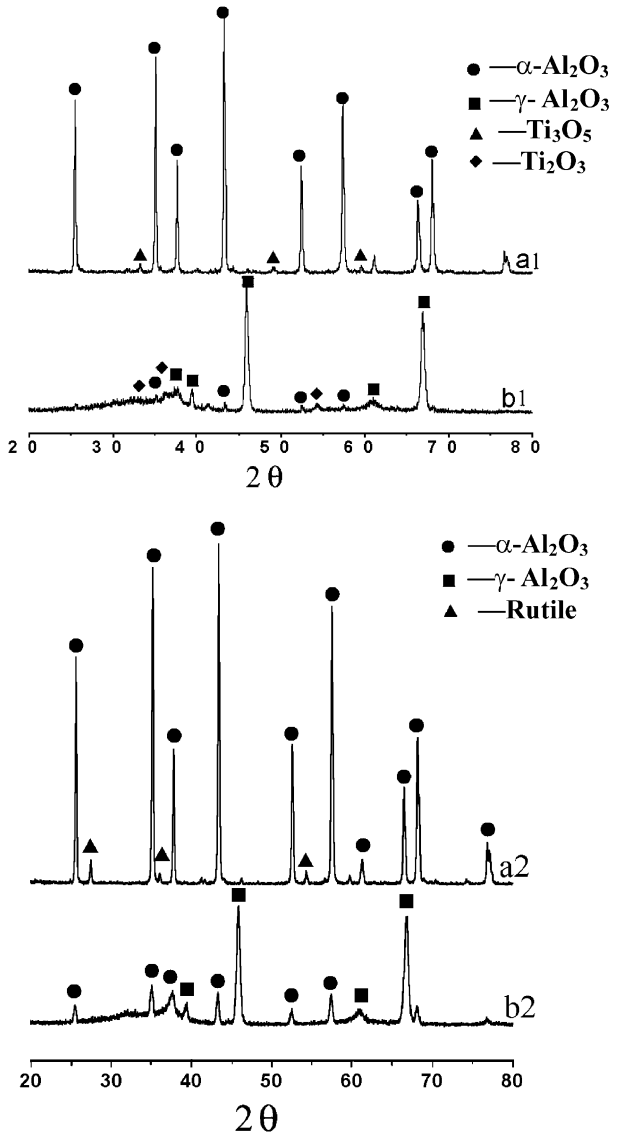

Fig. 2. X-ray diffraction patterns of the powders Al_2O_3–3 wt.% TiO_2 and as-sprayed coatings: (a1) conventional powder; (a2) nanostructured powder; (b1) conventional coating; (b2) nanostructured coating.

powders. Rutile phase of TiO_2 was found in the nanostructured powder. However, only Ti_3O_5 appeared in the conventional powder, which was formed during the fusing and crushing process. It can be seen that both nanostructured and conventional coatings predominantly contained the defective spinel cubic γ-Al_2O_3. In view of the nucleation kinetics, McPherson[13] suggested that γ-Al_2O_3 tended to be nucleated from the melt in preference to α-Al_2O_3 at the high cooling rate because of lower interfacial energy between crystal and liquid. But, there were also some differences in the XRD patterns of both coatings. The ratio of the heights of $\{13\}\alpha$ and $\{440\}\gamma$ peaks in the nanostructured coating was higher than in the conventional coating, indicating that the nanostructured coating contained more α-Al_2O_3. Due to high porosity of agglomerated particulates, heat dissipation increases and heat conduction is reduced, resulting in the decrease of the degree of granule melting during plasma spraying.[14] It has been recognized that the more the fraction of partially melted particles are, the higher the content of α phase after plasma spraying.[15] Thus, the increase of α-Al_2O_3 in the nanostructured coating may be relative to the decrease of the melting degree of feedstock. In addition, the peaks of TiO_2 disappeared from the XRD spectrum of the nanostructured coating. For the conventional coating, titania existed in the modification of Ti_2O_3 derived from Ti_3O_5 that was further deoxidized during the plasma spraying process. According to Normand's opinion,[16] the total contact surface area between alumina and titania is higher in the nanostructured powders than that in the conventional powders because of the small size of nanosized particles. In the nanostructured coating, TiO_2 nearly reacted with Al_2O_3 completely during plasma spraying to form solid solution χ-Al_2O_3·TiO_2 in the nanostructured $Al2O_3$–3 wt.% TiO_2 powder under the nonequilibrium condition of the plasma-spray process.[17,18]

3.2. Microstructure of coatings

Fig. 3 depicts the typical surface topographies of the plasma sprayed coatings. The conventional Al_2O_3–3 wt.% TiO_2 coating exhibited definite splat morphologies with densely packing splats (pancake-like). For the nanostructured Al_2O_3–3 wt.% TiO_2 coating, the splats were also present but many spherical particles existed on the surface. Agglomerated powders burst during pneumatic transport because of poor mechanical resistance.[14] As a result, many small particles existed in the nanostructured coating due to insufficient impact momentum.

The cross-sectional morphologies of the as-sprayed coatings are shown in Fig. 4. From the cross-sectional microstructures, it can be seen that both coatings consist of the lamella built up from the molten droplets impinging on the substrate. The composition contrast from backscattered electron micrographs illustrated that the nanostructured Al_2O_3–3 wt.% TiO_2 coating possessed a more homogeneous structure, but the conventional coating presented a distinct layered structure, i.e. aluminum-rich regions (gray) separated from titanium-rich regions (white). There were more small and spherical pores for the nanostructured Al_2O_3–3 wt.% TiO_2 coating than that for the conventional Al_2O_3–3 wt.% TiO_2 coatings, as indicated by arrows. According to image analysis, it was calculated that the porosities are 6 and 8% for the conventional and nanostructured Al_2O_3–3 wt.% TiO_2 coatings, respectively. The increase in porosity of the nanostructured coating may result from low density and high gas content of spray dried granules which remains when the granules are deposited during the plasma spraying process.[19]

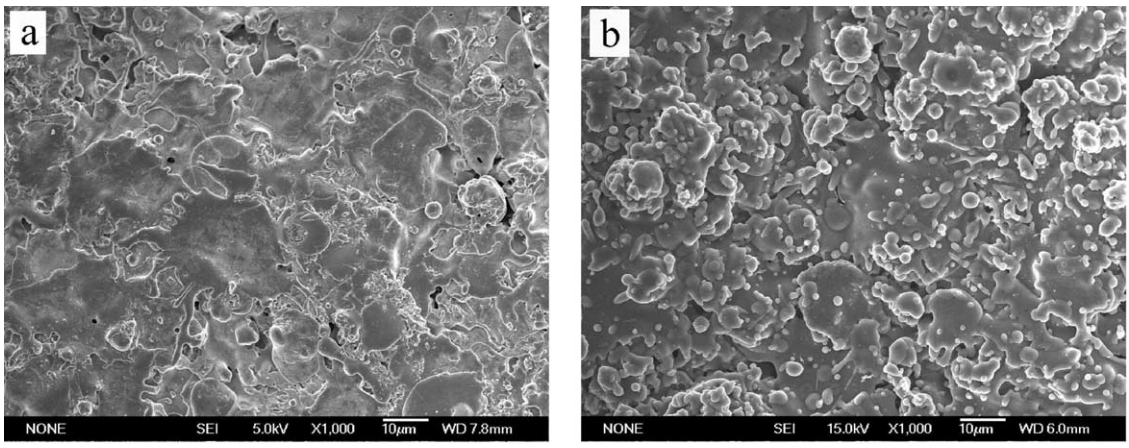

Fig. 3. Scanning electron micrographs of the surfaces of the as-sprayed Al_2O_3–3 wt.% TiO_2 coatings: (a) conventional; (b) nanostructured.

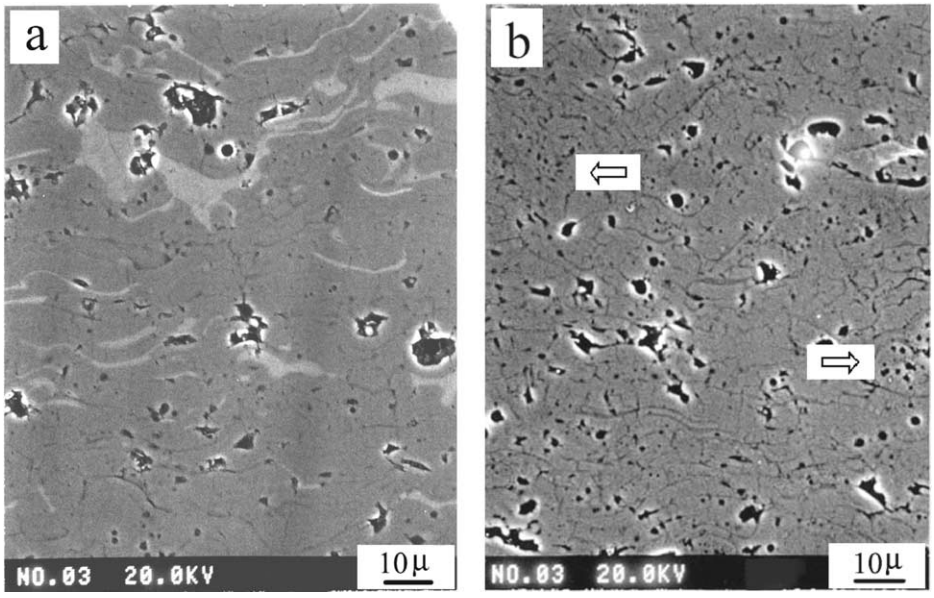

Fig. 4. Cross-sectional morphologies of the as-sprayed Al_2O_3–3 wt.% TiO_2 coatings: (a) conventional; (b) nanostructured.

Fig. 5 presents SEM micrographs of fracture surfaces of the as-sprayed coatings perpendicular to the substrate surface. The conventional Al_2O_3–3 wt.% TiO_2 coating exhibited a typical lamellar structure, indicating that the conventional powders were melted and spread well during plasma spraying. However, a composite microstructure was observed in the nanostructured Al_2O_3–3 wt.% TiO_2 coating, as shown in Fig. 5b. Namely, the nanostructured coating not only possessed the splat lamellae, which was similar to the conventional coating, but also contained equiaxed grains within splats, which size were in the range of 150 to 700 nm. Equiaxed grains were also observed in the nanostructured coating by TEM analysis, as shown in Fig. 6a. The selected area diffraction (SAD) revealed that the equiaxed grains were α-Al_2O_3 phase. Combining the SEM and TEM observations, it was inferred that equiaxed α-Al_2O_3 grains were originated from the partially melted or unmelted nanostructured powder. It is well known that plasma spraying is a fast process, the velocity of plasma jet is as high as 200 $m \cdot s^{-1}$ and the residence time of powders inside the plasma jet is less than 10^{-3} s.[20] Thus nano-sized alumina grains in the partially melted or unmelted nanostructured powder had little time to grow up during plasma spray process, and finally were embedded in the coatings. However, the major structures observed in TEM examination were columnar grains, as shown in Fig. 6b. And, the diameter of the elongated grain mostly ranged from 20 to 200 nm. The analysis of SAD patterns showed that these columnar grains were γ-Al_2O_3. It has been reported that the diameter of the columnar grains is mostly between 100 and 400 nm and α-Al_2O_3 grains are even of up to several micrometers in size in thick plasma sprayed alumina coatings ($\geqslant$200 μm).[21,22] Thus, the grain size of the nanostructured Al_2O_3–3 wt.% TiO_2 coating was smaller

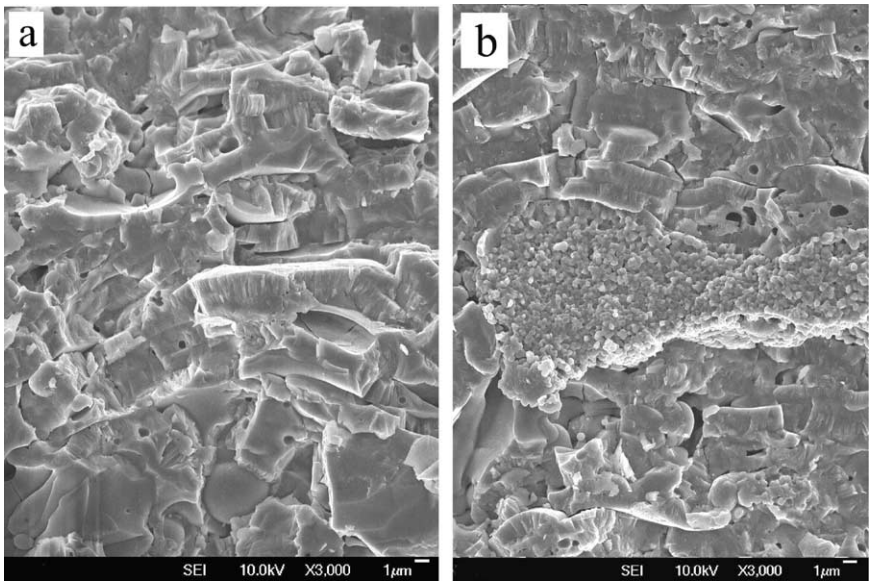

Fig. 5. SEM micrographs of fracture surface of the as-sprayed Al_2O_3–3 wt.% TiO_2 coatings: (a) conventional; (b) nanostructured.

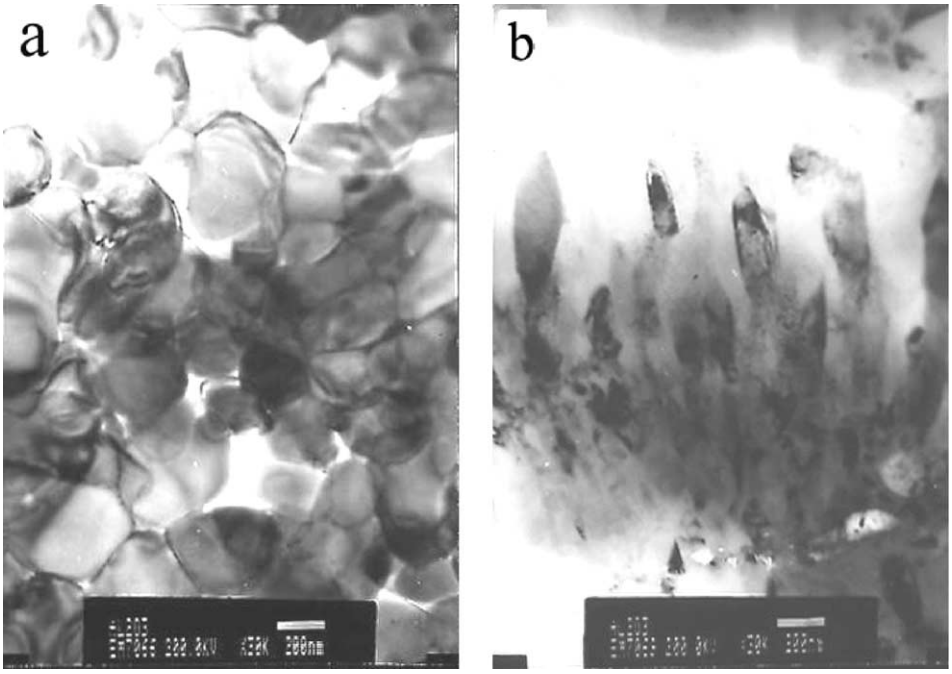

Fig. 6. TEM micrographs of the nanostructured Al_2O_3–3 wt.% TiO_2 coating: (a) α- Al_2O_3; (b) γ- Al_2O_3.

than that of the conventional coating. It is assumed that the decrease in grain size may contribute to the improvement of mechanical properties of the nanostructured coating.

3.3. Morphology of indentation cracks and mechanical properties

Fig. 7 presents the typical optical micrographs of the indentation cracks in the as-sprayed coatings at the load of 1000 gf. From Fig. 7, it can be seen that the indentation cracks preferentially propagated in the direction parallel to the substrate surface. This is due to the weak cohesion between splats in the plasma sprayed ceramic coatings,[12,23] where there is limited real contact between the rapidly solidifying splats and the actual area of contact has been estimated at only around 20%.

It is convenient to express fracture toughness of the plasma sprayed coatings using the crack extension force

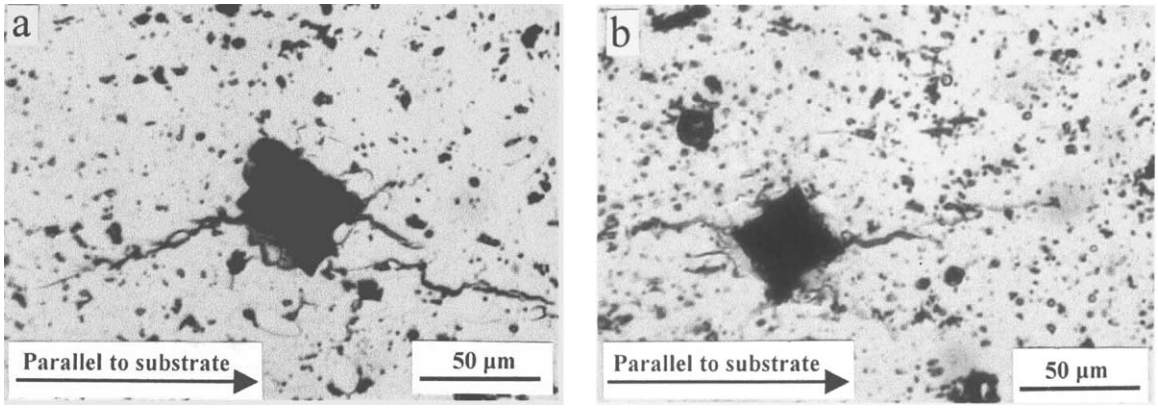

Fig. 7. Optical micrographs of indentation cracks in the as-sprayed Al_2O_3–3 wt.% TiO_2 coatings: (a) conventional; (b) nanostructured.

(G_C), which is proportional to fracture toughness and can be calculated in terms of the following Eq. (1):[12]

$$G_C = 6.115 \times 10^{-4} \cdot a^2 \cdot P/c^3 \quad (1)$$

where G_C = crack extension force, a = impression half-diagonal, c = the crack length measured from the center of the indentation, and P = intention load. The measured microhardness and crack extension force values for both conventional and nanostructured Al_2O_3–3 wt.% TiO_2 coatings were the average values of 20 tests. Microhardness of the nanostructured coating was similar to that of the conventional coating and about 820 $HV_{0.2}$. The adhesion strength and crack extension force of the nanostructured coating were 22.9 MPa and 8.5 $J{\cdot}m^{-2}$. For the conventional coating, they were 16.7 MPa and 4.7 $J{\cdot}m^{-2}$. The results obtained indicated that the adhesion strength and crack extension force of the nanostructured coating increased by 33 and 80%, respectively.

The residual stresses resulting from the anisotropy of elastic and thermal expansion properties can weaken the grain boundary strength[24,25] and have important effect on the adhesion strength of the thermal sprayed coatings.[26] The stresses can be relaxed by plastic deformation. With grain size decreasing, the plasticity of ceramics increases because the grain boundary diffusion is enhanced by the high concentration of grain boundaries.[27] In the nanostructured Al_2O_3–3 wt.% TiO_2 coating, plastic deformation provided a process for energy dissipation and reduced the stresses due to the existence of equiaxed nano-sized α-Al_2O_3 grains and the decrease of γ-Al_2O_3 grain size, which resulted in higher adhesion strength between splats and substrate and/or the previous deposited layers. Additionally, the heterogeneous structure, i.e. alumina and titania separated each other can result in weak stratification.[28] The improvement of the adhesion strength of the nanostructured Al_2O_3–3 wt.% TiO_2 coating may be partly attributed to the more homogenous structure resulting from the solid solubility between alumina and titania.

The toughness of the plasma sprayed coatings is relative to the adhesion strength between splats and substrate and/or the previous deposited layers.[28] Cracks are propagated along the splat boundaries, as shown in Fig. 7. Because of weak inter-splat bonding, the toughness of the plasma sprayed alumina coating was decreased by 50% compared with that of sintered aluminas. Toughness of the coatings can be improved by increasing the cohesion/adhesion strength, which accounted for increasing the toughness of the nanostructured Al_2O_3–3 wt.% TiO_2 coating. It has been recognized that the fracture strength of some oxide ceramics can be increased by a factor of 1.5–3 by adding fine inclusions.[29] The presence of equiaxed α-Al_2O_3 grains in γ-Al_2O_3 matrix may be also beneficial to the improvement of the toughness of nanostructured Al_2O_3–3 wt.% TiO_2 coating. Thus, it was concluded that the improvement of mechanical properties of the nanostructured Al_2O_3–3 wt.% TiO_2 coating resulted from the changes in microstructure, i.e. the solid solubility between alumina and titania, the existence of equiaxed α-Al_2O_3 grains and the decrease of γ-Al_2O_3 grain size.

Fig. 8 gives the friction coefficient and wear rate of both nanostructured and conventional Al_2O_3–3 wt.% TiO_2 coatings mated to steel balls as sliding pairs at room temperature and under dry condition. From Fig. 8a, it can be seen that the friction coefficients of the conventional and nanostructured Al_2O_3–3 wt.% TiO_2 coatings were similar and about 0.51. However, the nanostructured coating had far lower wear rate than that of the conventional coating (Fig. 8b) It has been pointed out that wear resistance of the plasma sprayed coatings show a high dependence on hardness and toughness.[16,30] In this case, the hardness of the conventional and nanostructured Al_2O_3–3 wt.% TiO_2 coatings was similar. Thus, the improvement of wear resistance of the nanostructured Al_2O_3–3 wt.% TiO_2 coating can be explained by the increase of toughness.

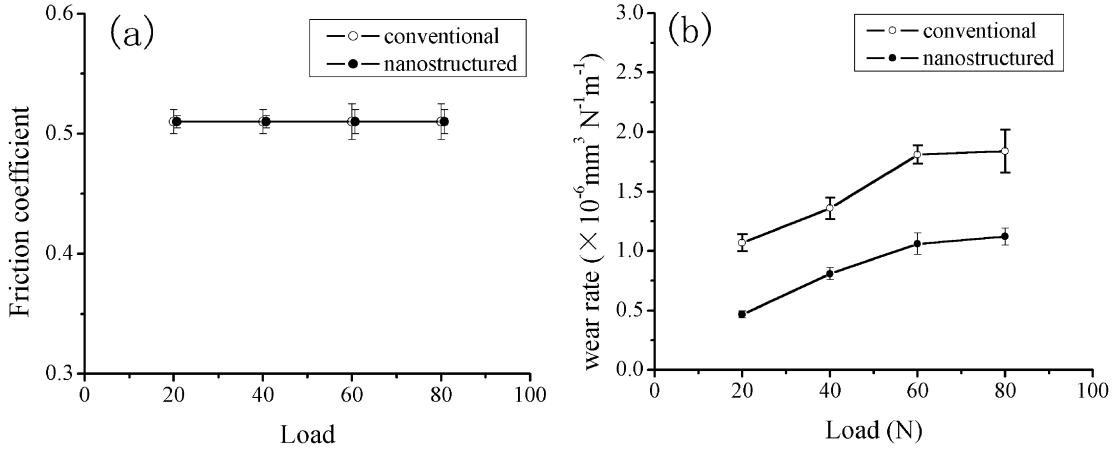

Fig. 8. Friction coefficient (a) and wear rate (b) of the as sprayed Al_2O_3–3 wt.% TiO_2 coatings as a function of load: (○) conventional; (●) nanostructured.

4. Conclusions

Nanostructured and conventional Al_2O_3–3 wt.% TiO_2 coatings were deposited by atmospheric plasma spraying. Microstructure and some mechanical properties of the as-sprayed coatings were characterized. Compared with the conventional coating, the nanostructured coating contained both equiaxed α-Al_2O_3 with size between 150 and 700 nm and γ-Al_2O_3 grains, most of which was less than 200 nm in size. Moreover, the nanostructured coating possessed a more homogeneous microstructure and TiO_2 phases disappeared in this coating, which is due to the reaction between nanosized TiO_2 and Al_2O_3 particles during plasma spraying. The microhardness values of the conventional and nanostructured Al_2O_3–3 wt.% TiO_2 coatings were similar. However, the adhesion strength and crack extension force of the nanostructured coating were 22.9 MPa and 8.5 $J{\cdot}m^{-2}$ respectively, which were about 1.3 and 1.8 times of the conventional coating. In addition, the nanostructured coating possessed an improved wear resistance.

Acknowledgements

The authors wish to express their thanks to Engineer Xiaming Zhou for preparing the coatings used in this study.

References

1. Rittner, M., Nanostructured materials: a technical-market analysis. *Indust. Ceram.*, 2000, **20**, 180–182.
2. Kim, B. K., Ha, G. H., Lee, G. G. and Lee, D. W., Structure and properties of nanophase WC/Co/VC/TaC hardmetal. *Nanostruct. Mater.*, 1997, **9**, 233–236.
3. Jia, K. and Fischer, T. E., Sliding wear of conventional and nanostructured cemented carbides. *Wear*, 1997, **203–204**, 310–318.
4. Sterns, L. C., Zhao, J. H. and Harmer, P., Processing and microstructure development in Al_2O_3–SiC nanocomposite. *J. Eur. Ceram. Soc.*, 1992, **10**, 473–477.
5. Weertman, J. R., Farkas, D., Hemker, K., Kung, H., Mayo, M., Mitra, R. and Van Swygenhoven, H., Structure and mechanical behavior of bulk nanocrystalline materials. *MRS Bulletin*, 1999, **24**(2), 44–50.
6. Kear, B. H., Sakangi, P. K., Jain, M., Yao, R., Kaiman, Z., Skandan, G. and Mayo, W. E., Thermal sprayed nanostructured WC/Co hard coatings. *J. Therm. Spray Technol.*, 2000, **9**, 399–406.
7. Kear, B. H. and Strutt, P. R., Chemical processing and applications for nanostructured materials. *Nanostructured material. Nanostruct. Mater.*, 1995, **6**, 227–236.
8. Shaw, L. L., Goberman, D., Ren, R., Gell, M., Jiang, S., Wang, Y., Xiao, T. D. and Strutt, P., The dependency of microstructure and properties of nanostructured coatings on plasma spray conditions. *Surf. Coat. Technol.*, 2000, **130**, 1–8.
9. Zhu, Y., Yukimura, K., Ding, C. and Zhang, P., Tribological properties of nanostructured and conventional WC-Co coatings deposited by plasma spraying. *Thin Solid Film*, 2001, **388**, 277–282.
10. Chen, H. and Ding, C. X., Nanostructured Zirconia coating prepared by atmospheric plasma spraying. *Surf. Coat. Technol.*, 2002, **150**, 31–36.
11. Guilemany, J. M., Nutting, J. and Dougan, M. J., A transmission electron microscopy study of the microstructures present in alumina coatings produced by plasma spraying. *J. Therm. Spray Technol.*, 1997, **6**, 425–429.
12. Ostojic, P. and McPherson, R., Indentation toughness testing of plasma sprayed coatings. *Mater. Forum*, 1987, **10**, 247–254.
13. McPherson, R., On the formation of thermally sprayed alumina coatings. *J. Mater. Sci.*, 1980, **15**, 3141–3149.
14. Denoirjean, A., Vardelle, A., Lugscheider E., Rass, I., Chandler, P., Mclntyre, R., Cosack, T. and Heijen, H.L., Comparison of the properties of plasma sprayed stabilized zirconia coatings for different powder morphologies. In *Proceedings of the International Thermal Spray Conference & Exposition*, Orlando, Florida, USA, 1992, pp. 967–973.
15. Ding, C. X., Zatorski, R. A. and Herman, H., Oxide powders for plasma spraying—the relationship between powder characteristics and coating properties. *Thin Solid Films*, 1984, **118**, 467–475.
16. Normand, B., Fervel, V., Coddet, C. and Nikitine, V., Tribo-

logical properties of plasma sprayed alumina-titania coatings: role and control of the microstructure. *Surf. Coat. Technol.*, 2000, **123**, 278–287.
17. Kear, B. H., Kalman, Z., Sadangi, R. K., Skandan, G., Colaizzi, J. and Mayo, W. E., Plasma-sprayed nanostructured Al_2O_3/TiO_2 powders and coatings. *J. Therm. Spray Technol.*, 2000, **9**, 483–487.
18. Goberman, D., Sohn, Y. H., Shaw, L., Jordan, E. and Gell, M., Microstructure development of Al_2O_3–13 wt.% TiO_2 plasma sprayed coatings derived from nanocrystalline powders. *Acta. Mater.*, 2002, **50**, 1141–1152.
19. Pekshev, P. Yu. and Murzin, I. G., Modelling of porosity of plasma sprayed materials. *Surf. Coat. Technol.*, 1993, **56**, 199–208.
20. Zhu, Y., Ding, C., Yukimura, K., Xiao, T. D. and Strutt, P. R., Deposition and characterization of nanostructured WC-Co coating. *Ceram. Internal.*, 2001, **27**, 669–674.
21. Heintze, G. N. and Uematsu, S., Preparation and structures of plasma-sprayed γ- and α-Al_2O_3 coatings. *Surf. Coat. Technol.*, 1992, **50**, 213–222.
22. Dutton, R., Wheeler, R., Ravichandran, K. S. and An, K., Effect of heat treatment on the thermal conductivity of plasma-sprayed thermal barrier coatings. *J. Therm. Spray Technol.*, 2000, **9**, 204–209.
23. McPherson, R., A review of microstructure and properties of plasma sprayed ceramic coatings. *Surf. Coat. Technol.*, 1989, **39–40**, 173–181.
24. Blendell, J. E. and Coble, R. L., Measurement of stress due to thermal expansion anisotropy in Al_2O_3. *J. Am. Ceram. Soc.*, 1982, **65**, 174–178.
25. Cho, S., Hockey, B. J., Lawn, B. R. and Bennison, S. J., Grain size and *R*-curve effects in abrasive wear of alumina. *J. Am. Ceram. Soc.*, 1989, **72**, 1249–1252.
26. McPherson, R., The relationship between the mechanism of formation, microstructure and properties of plasma-sprayed coatings. *Thin Solid Film*, 1981, **83**, 297–310.
27. Edelstein, A. S., Murday, J. S. and Rath, B. B., Challenges in nanomaterials design. *Prog. Mater. Sci.*, 1997, **42**, 5–12.
28. Beltzung, F., Zambell, G. and Lopez, E., Fracture toughness measurement of plasma sprayed ceramic coatings. *Thin Solid Films*, 1989, **181**, 407–415.
29. Niihara, K. and Nakahira, A., Strengthening of oxide ceramics by SiC and Si_3N_4 dispersions. In *Proceedings of the Third International Symposium on Ceramic Materials and Components for Engines*, American Ceramic Society, Westeville, OH, 1988, pp. 919–926.
30. Erickson, L. E., Hawthorne, H. M. and Troczynski, T., Correlations between microstructural parameters, micromechanical properties and wear resistance of plasma sprayed ceramic coatings. *Wear*, 2001, **250**, 569–575.